ANNALS OF GEOPHYSICS, VOL. 45, N. 5, October 2002

Source characteristics of a moderate earthquake (*M* 4.9) using empirical Green's function technique

Ali K. Abdel-Fattah
National Research Institute of Astronomy and Geophysics, Helwan, Cairo, Egypt

Abstract
The rupture process of a moderate earthquake (*M* 4.9) on 28th January 1999 was analyzed using velocity records at local distances less than 80 km. The characterization of the rupture process was obtained from studying aftershocks distribution, azimuthal variations of Relative Source Time Functions (RSTFs), and a set of spatio-temporal slip models. RSTFs were retrieved by deconvolution of small aftershock records from those of the mainshock. In addition, velocity *P*-wave records of the respective event were inverted to recover slip distribution on the fault plane using the records of aftershocks as Empirical Green Functions (EGFs). The waveform inversion was adopted using three EGFs. In the inversion, the rupture propagation velocity was fixed and assumed to be eight-tenths of the local shear wave velocity. The total seismic moment was estimated to range from 0.011 E + 18 Nm (M_w = 4.6) to 0.017 E + 18 Nm (M_w = 4.8). The hypocentral distribution of the aftershocks, azimuthal variations of RSTFs, and the set of slip distribution models were exhibited bilateral rupture propagation along the strike and dip of the fault plane. The presence of two to three high slip patches on the fault plane suggested that a complex rupture pattern is detectable for a moderate size earthquake. However, the so-called nucleation phase was invisible in the present analysis.

Key words *empirical Green's function – aftershocks distribution – relative source time function – spatio-temporal slip models*

1. Introduction

The description of earthquake rupture histories is crucial not only to understand the physical processes of earthquake generation but also to predict strong motions of large earthquakes. Detailed studies of earthquake rupture processes revealed that rupture begins with a relatively low moment rate before it propagates dynamically. This idea was introduced by theoretical models (*e.g.*, Andrews, 1976; Das and Scholz, 1981; Dieterich, 1986, 1992; Shibazaki and Matsu'ura, 1998) and laboratory experiments (*e.g.*, Dieterich, 1979; Ohnaka *et al.*, 1987) to simulate the initial stage of earthquakes. Theoretical and experimental results indicated that slip initiates and accelerates gradually within a small finite part of the entire fault before the dynamic rupture occurs. Recently, many seismological studies have described the behavior of earthquake initiations. For example, Brune (1979) concluded that the initiation of large earthquakes is similar to that of small events. Umeda (1990, 1992) reported the existence of a low amplitude initial phase preceding the main *P*-phase in large earthquakes. Iio (1992, 1995) observed this view for micro-earthquakes of Nagano prefecture. Abercrombie and Mori (1994) explained that the beginning of the *M* 7.3 Landers, California earthquake was similar to an

Mailing address: Dr. Ali K. Abdel-Fattah, National Research Institute of Astronomy and Geophysics, Helwan 11421, Cairo, Egypt; e-mail: ali_kamel@yahoo.com

aftershock of *M* 4.4. Anderson and Chen (1995) showed that no systematic difference was observed in the *P*-wave initiation of *M* 3.0-*M* 8.0 events in Michoaca, Mexico. Furthermore, Mori and Kanamori (1996) supported that earthquakes of all sizes initiate in a similar manner and begin to grow dynamically within a few hundredths of seconds after the rupture initiation. Ellsworth and Beroza (1995) showed that the Hector Mine earthquake exhibited rupture complexities similar to large earthquakes. They pointed out that the Hector Mine earthquake started with about a 1.8 s foreshock or nucleation phase followed by the main rupture.

The imaging of earthquake slip histories might enhance our understanding of earthquake physical processes. Fletcher and Spudich (1998) inverted the source time functions of moderate earthquakes into slip distribution and rupture time to infer fault properties of the initiation zone at Parkfield. They analyzed three earthquakes of complex slip histories started at a small spike and then expanded into the largest patch. Such studies for small to moderate earthquakes require good quality of near-field observation records. On the 28th January 1999, the Earthquake Research Institute (ERI) seismic network stations, Tokyo University recorded an earthquake of magnitude 4.9 and its aftershocks that took place in Nagano prefecture. This earthquake sequence yielded many good waveform records, which provided an opportunity to determine the slip distribution in space and time.

In the present study, the deconvolution technique in the time domain was applied to retrieve RSTFs using velocity records of aftershocks as EGFs. In a second step, the most appropriate EGFs were used to invert the waveform data and recover the spatio-temporal slip distribution on the fault plane. Results were interpreted in terms of rupture complexities. All analyses were confined to the first few seconds of the *P*-wave records.

2. Data

To investigate the slip history of a moderate earthquake using EGFs, a magnitude 4.9 event of the Japanese earthquakes was chosen. The respective event was followed by aftershocks with a range of magnitudes 1.5 to 4.0 and all were recorded by nearby seismic stations of the ERI seismic network (fig. 1). All instruments are 1 Hz velocity sensors with a dynamic range 24-bit digital recording system and a sampling rate of 100 samples per second. In addition to ERI permanent seismic stations, four portable seismic stations were installed close to the mainshock to locate aftershocks accurately. The error in aftershock locations is less than 100 m in width and 200 m in depth. Figure 2 shows the distribution of aftershock hypocenters determined by the ERI. The location of the mainshock and of three EGFs is shown in fig. 3. The capital letters M, AF1, AF2 and AF3 correspond respectively to mainshock and aftershocks as listed in table I. Appropriate EGFs were selected by examining aftershocks with magnitude nearly 2 units smaller than that of the mainshock. The appropriate aftershocks were chosen on the basis of their high signal to noise ratio.

3. Method

Briefly, two steps were used in the present study. The first step was to extract RSTFs by deconvolution of EGFs records from those of the respective event. In the second step, three appropriate EGFs were used to invert the waveform data and obtain the slip history on the fault plane using the method of Ide and Takeo (1997).

3.1. *Empirical Green's function*

Detailed investigations of earthquake source processes require good knowledge of the effects of path, site and instrument responses. By considering seismic records of small earthquakes located close to a larger one, the forementioned effects would be available using small events as EGFs. For two earthquakes with different sizes but having similar hypocenters and focal mechanisms, one can treat the waveform of the smaller event as an EGF and deconvolve it from the larger event to obtain the RSTF of the larger earthquake (Mueller, 1985). Since the pair of events is recorded at the same station by the same

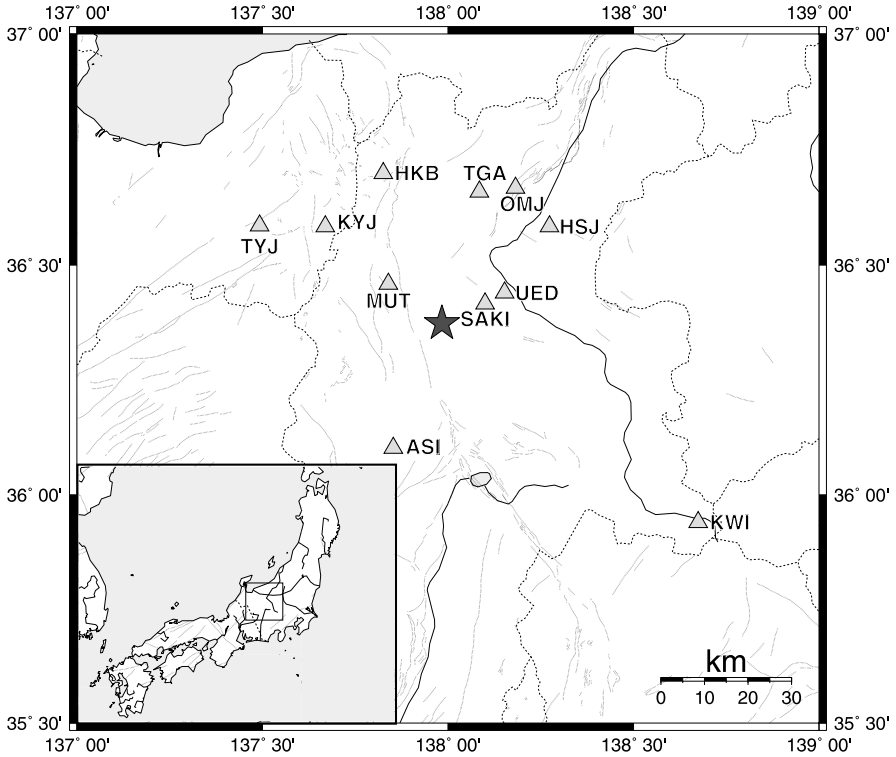

Fig. 1. Locations of the 28th January 1999 Nagano earthquake (solid star) and ERI seismic stations used in the deconvolution and waveform inversion processes

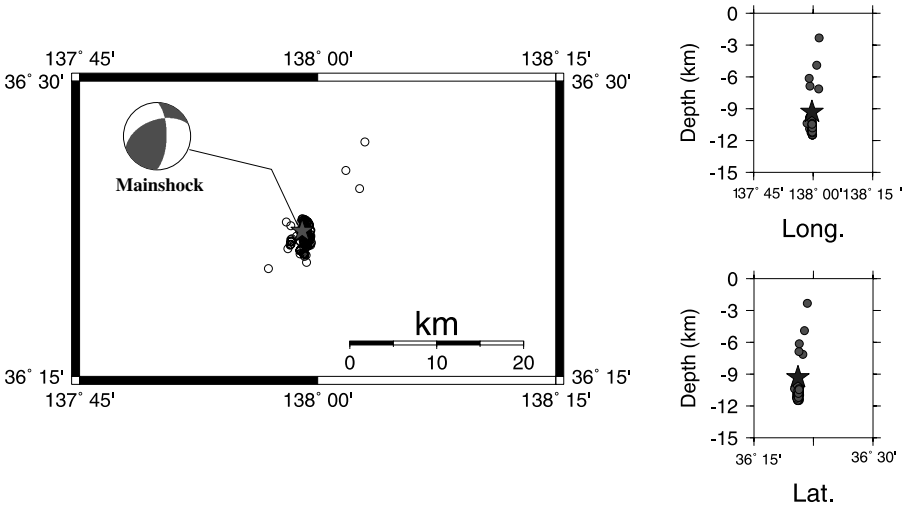

Fig. 2. Focal mechanism of the mainshock, epicentral and hypocentral distribution of mainshock (solid star) and aftershocks (open circles)

Table I. The focal parameters of mainshock and EGF aftershocks.

ID	Date	Origin time	Lat. (°)	Long. (°)	Depth (km)	M_{JMA}*
M	99.01.28	10:25:48.40	36.3733	137.9837	09.3	4.9
AF1	99.01.28	11:05:38.40	36.3699	137.9920	11.5	2.9
AF2	99.01.28	11:41:11.70	36.3730	137.9899	11.3	2.7
AF3	99.01.28	11:59:27.90	36.3790	137.9891	11.4	2.8

*M_{JMA} denotes the magnitude determined by the Japan Meteorological Agency (JMA).

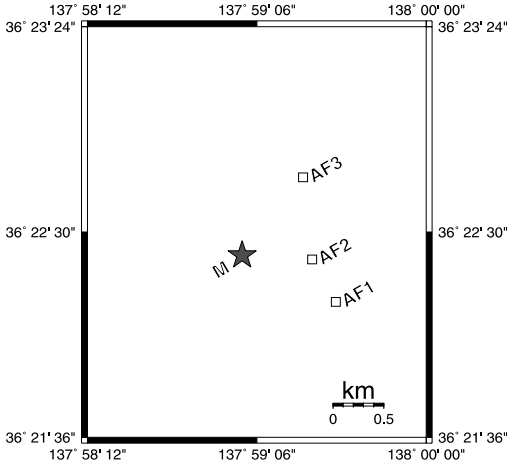

Fig. 3. Epicentral locations of EGF's (open squares) used in deconvolution and waveform inversion with respect to the mainshock location (solid star).

instrument and has almost the same propagation path, the deconvolution process should result in an RSTF that is corrected for the path, site and instrument effects.

Since Hartzell (1978) proposed an EGF method to estimate synthetic seismograms, many researchers have applied and developed this method (*e.g.*, Kanamori, 1979; Hadly and Helmberger, 1980; Irikura and Muramatu, 1982; DiBona and Boatwright, 1989). The EGF deconvolution technique has been used to extract RSTFs for small earthquakes to estimate the earthquake source parameters (*e.g.*, Frankel *et al.*, 1986; Li and Thurber, 1988; Mori and Frankel, 1990; Xie *et al.*, 1991). RSTFs were also used to reveal rupture complexity and directivity (*e.g.*, Frankel *et al.*, 1986; Li and Thurber, 1988; Mori and Frankel, 1990; Abdel Fattah and Badawy, 2001). In this study, RSTFs were retrieved to examine rupture directivity and complexity of a moderate earthquake. RSTFs were obtained by applying the deconvolution technique in the time domain with non-negative constraints (Lawson and Hanson, 1974). The deconvolution was performed as a least square problem (Abdel Fattah and Badawy, 2001). As an example, fig. 4a-e shows the deconvolution procedure for the mainshock using the vertical component record of the UED station. A key assumption of using a small event as an EGF is that the source duration of its source time function is short compared to that of the larger event. Therefore, this small event can be considered as an impulsive source. Thus, the resulting RSTF reflects the source characteristics of the larger event. A cross-correlation analysis was performed to distinguish the waveform similarity between the mainshock and its aftershocks. The events having a good correlation to the mainshock were used as Green function events. After deconvolution, a Butterworth low-pass filter with a corner frequency of 30 Hz was applied to reduce the high-frequency noise of the retrieved RSTFs. The filtered RSTFs exhibited similarity in the pulse shapes for three cases of EGFs (fig. 5a-c). In order to confirm the appropriateness of the EGFs, three appropriate aftershocks were adopted. In addition, fig. 5a-c displayed that RSTFs were complex with narrow pulse widths toward north and south directions. The pulse duration of RSTFs was measured from the deconvolution delay time of EGF (0.8 s) to the first zero crossing. The pulse widths ranged from 0.27 to 0.6 s. Azimuth pulse width variations of the ob-

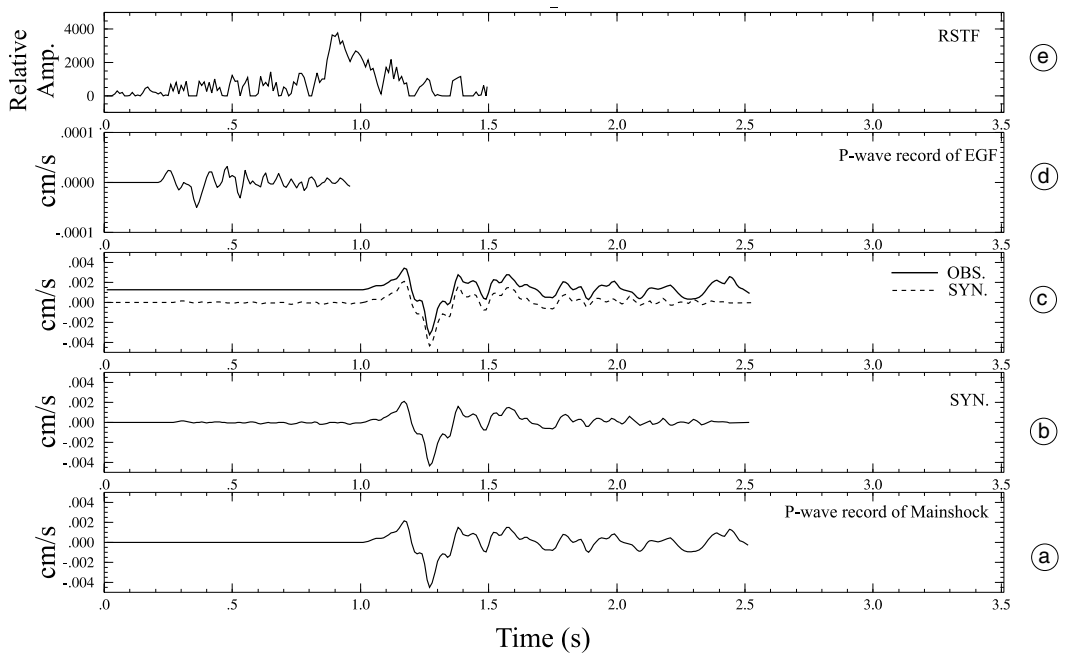

Fig. 4a-e. An example of the RSTF of the mainshock derived from *P*-waves by using the record of event AF1 as a Green's function at the UED station. a) The mainshock record. b) The convolution result of the RSTF with the record of EGF. c) The waveform data of the mainshock (solid line) and the result of the convolution of the RSTF with the record of EGF (dotted line). d) The record of AF1. e) The deconvolved RSTF.

tained RSTFs were a diagnostic of the rupture directivity. Variations of the RSTF pulse width with its station azimuth are shown in fig. 6a-c. The azimuthal variations of RSTF pulse widths showed that rupture propagates bilaterally. From fig. 6a-c, it was also obvious that the pulse widths were narrow at stations to the north and south. The advantage of the EGF deconvolution technique is that it allows investigation of rupture complexity and directivity.

3.2. *Determination of slip distribution*

Once the appropriate EGFs were determined, a simple EGF method was used to obtain the spatio-temporal slip distribution on an assumed fault plane. Various inversion methods have been developed to determine spatio-temporal distribution of slip on a fault plane from seismic waveform data (*e.g.*, Olson and Apsel, 1982; Hartzell and Heaton, 1983, 1986; Kikuchi and Fukao, 1985; Mori and Shimazaki, 1985; Yoshida, 1986, 1988; Kikuchi and Kanamori, 1986; Takeo and Mikami, 1987; Satake, 1989; Beroza and Spudich, 1988; Mori and Hartzell, 1990; Ide *et al.*, 1996). To express the total rupture process as a spatio-temporal slip distribution on a fault plane, the whole fault plane was divided into many subfaults and the slip was estimated at each subfault. The problem here was how to choose the dimensions of subfaults or the number of subdivisions. If the fault is divided into a small number of large subfaults, the solution will have poor resolution. Alternatively, if a large number of small subfaults are used, the inversion will be unstable and rapidly vary due to the noise contained in the data. The relation between the synthetic record at a station and the slip rate distribution $\dot{u}_i(x,t)$ on the fault plane is repre-

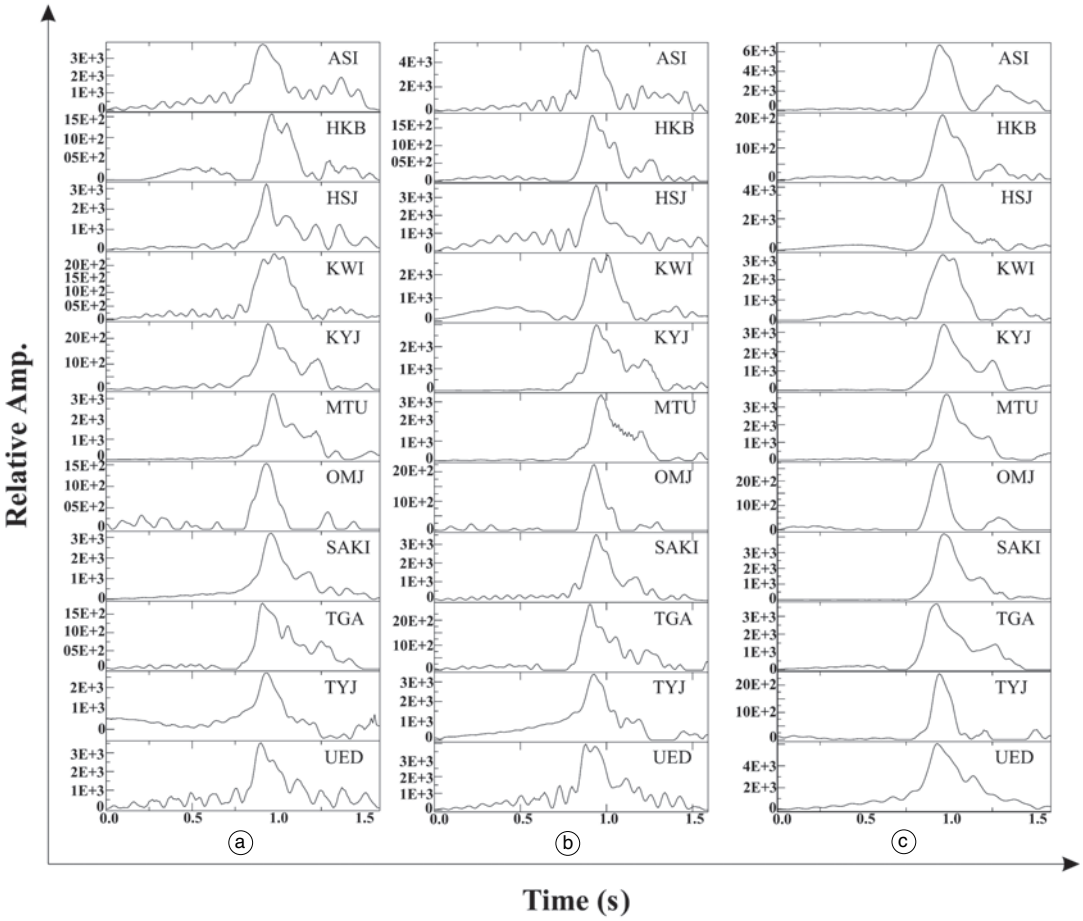

Fig. 5a-c. The obtained Relative Source Time Functions (RSTF's) for the mainshock using empirical Green's functions (EGFs) (a) AF1, (b) AF2 and (c) AF3, respectively.

sented as

$$U_j(x,t) = \int\int g_{ij}(x,t;\xi,\tau)\cdot \dot{u}_i(\xi,\tau)d\xi\, d\tau \quad (3.1)$$

where $g_{ij}(x,t,\xi,\tau)$ is an empirical Green's function representing the j^{th} component of velocity waveforms record at a station when an impulsive slip rate in the i^{th} direction is applied at $x = \xi$, $t = \tau$. Ide and Takeo (1997) expanded the spatio-temporal distribution of slip rate $\dot{u}_i(x_1, x_2, t)$ as

$$\dot{u}_i(x,t) = \sum a_{ilmn}\cdot \phi_l^1(x_1)\cdot \phi_m^2(x_2)\cdot \psi_n(t) \quad (3.2)$$

where, a_{ilmn} are expansion coefficients and $\phi^1_{\ l}(x_1)$, $\phi^2_{\ m}(x_2)$ and $\psi_n(t)$ are the basis function in strike direction, dip direction and time, respectively. In this study, each basis function is an isosceles triangle determined by three nodes, and hence the slip distribution is continuous everywhere spatially and temporally. Substituting (3.2) into (3.1), the observed displacement equation can be expressed as

$$U_j(x,t) = \sum a_{ijlmn}\int\int g_{ij}(x,t;\xi,\tau)\cdot \cdot \phi_l^1(\xi_1)\cdot \phi_m^2(\xi_2)\cdot \psi_n(\tau)d\xi\, d\tau \quad (3.3)$$

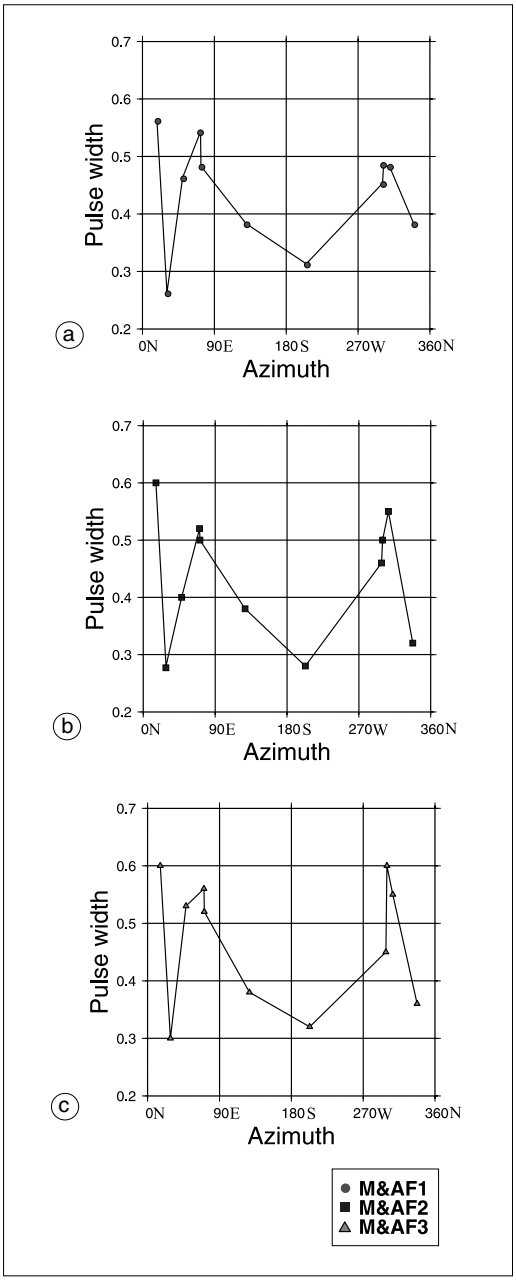

Fig. 6a-c. The distribution of RSTF (derived from deconvolution technique) pulse widths against station azimuths. a) Using the *P*-wave record of event AF1. b) Using the *P*-wave record of event AF2. c) Using the *P*-waves record of event AF3.

This equation can be written in vector form as

$$d = G \cdot m \qquad (3.4)$$

where d is the vector representing observed data, m is the model parameter vector of a_{ilmn}, and G is a N by M convolution matrix obtained by (3.4) with sampling corresponding to d. This linear inversion equation was solved by Bayesian modeling described in Ide *et al.* (1996). Two smoothing constraints were applied, spatial and temporal constraints, to minimize the difference between the coefficients of spatio-temporally neighbouring basis functions. The weights of the constraints were determined using Akaike's Bayesian Information Criterion (ABIC, Akaike, 1980). The Non-Negative Least-Square (NNLS) algorithm was employed (Lawson and Hanson, 1974). The approach of modeling large events with a summation of smaller ones has the advantage of simplicity, but its potential is limited by the fact that suitable empirical records are not always available.

3.3. *Preparation to inversion*

The slip is assumed to be distributed on the fault plane whose geometry is determined from the focal mechanism solution in combination with aftershock distributions. Figure 2 shows the ERI focal mechanism solution determined using the moment tensor inversion. The focal mechanism solution indicated reverse faulting with a strike-slip component. The plane striking N-S and dipping to the east is constrained with the aftershock distribution and selected as the fault plane. Following Ide and Takeo (1997), a seismic source model could be represented as a spatio-temporal distribution of slip which expanded by triangle shaped basis functions arranged along the two dimensional fault plane (strike and dip) and along the time axis. The unknown parameters are coefficients of the basis functions. The numbers of the basis functions are 9, 9 and 7 in the strike, dip and time, respectively. Node intervals are 0.25 km in the strike, 0.25 km in the dip and 0.02 s in the time. The total source duration is about 0.16 s. The total number of model parameters used in inversion is 567. The central point on the assumed fault represents the initiation

Table II. Velocity structure used in this study.

P-velocity (km/s)	*S*-velocity (km/s)	Depth (km)	Density
5.5	3.09	0.0	2.5
6.1	3.43	4.5	2.7
6.7	3.76	15.0	3.0
8.0	4.49	32.0	3.2

point of the rupture. In the linear inversion, we assumed a fixed rupture velocity of 2.7 km/s which determines the start time for a basis function at each point on the fault plane from the hypocenter. The travel times from each subfault to observers are calculated using a layered crustal structure shown in table II.

4. Results and discussion

The development of waveform inversion methods revealed that source processes of the large earthquakes are generally complex (*e.g.*, Hartzell and Heaton, 1983; Beroza and Spudich, 1988; Takeo, 1988; Waled and Heaton, 1994; Ide *et al.*, 1996). For small earthquakes, Tsukuda (1980) carefully analyzed the *P*-waveforms of events with *M* 1-2 and showed that their sources were represented by a simple fault model. Recently, detailed analysis of seismic sources also indicated that source processes of small to moderate earthquakes are apparently similar to those reported for large earthquakes. Nishigami (1987) analyzed several earthquake groups and observed that earthquakes with $M \geq 2.5$-3.0 showed complicated *P*-waveforms (multiple shocks composed of two or three subevents). Mori and Frankel (1990) determined source time functions for small earthquakes ($M_L = 1.7$ to 4.4) using an EGF approach and showed that some of them exhibited significance pulse shapes suggesting more complex ruptures. Li *et al.* (1995) determined the STF for $M_N = 1.2$ to 4.4 earthquakes in the Charlevoix seismic zone, Quebec, Canada by employing an empirical Green's approach. They used the STF pulse amplitudes as a function of station azimuths to estimate the rupture directions and the rupture velocities. They showed rupture complexities in an earthquake of magnitude 3.3. The rupture complexities of micro-earthquakes in Miramichi, Canada ($M \sim 3$ to 4.1) and in Eastern Maine (16 September 1994, $M = 3.9$) were also observed from retrieved RSTFs (Li *et al.*, 1994, 1995). Ide (2001) determined a set of detailed source models of 18 moderate earthquakes (*M* 4-5), representing a part of the swarm activity beneath the Hida-Mountains in Central Japan in 1998, using a waveform inversion procedure of the EGF. The rupture process of these earthquakes is complex and is apparently similar to the rupture process in large earthquakes. Further, Abdel-Fattah and Badawy (2002) retrieved complex source time functions, using empirical Green's function, of the October 11, 1999 earthquake ($M_L \sim 4.9$) occurring in Southeast Beni-Suef, Northern Egypt.

In the present study, a simple EGF method was used to reveal the rupture process of a moderate earthquake. The obtained RSTFs and the set of spatio-temporal slip distribution models on the fault plane were used to describe the rupture complexity of the respective event. Three different appropriate aftershocks were adopted to obtain RSTFs and slip models and to evaluate the validity and applicability of the empirical Green's function method. RSTFs were obtained by EGF deconvolution technique in time domain. On other hand, the slip distribution was expanded by basis functions and the unknown parameters are the expansion coefficients of these functions (Ide and Takeo, 1997). The model parameters were determined using the non-negative least squares algorithm of Lawson and Hanson (1974). The difference between the coefficients of the spatio-temporally basis functions is minimized by Bayesian modeling constrains described by Ide *et al.* (1996).

On the basis of the obtained slip models and RSTFs as well as aftershock distribution, the source processes of our respective earthquake were defined. The rupture was roughly propagated bilaterally along the strike and dip of the fault plane. The spatio-temporal distribution of source time functions for each subfault along the fault plane is shown in fig. 7a. The result of the inversion for the set of slip distribution models is shown in fig. 7b. E01, E02 and E03 represent the slip models using AF1, AF2 and AF3,

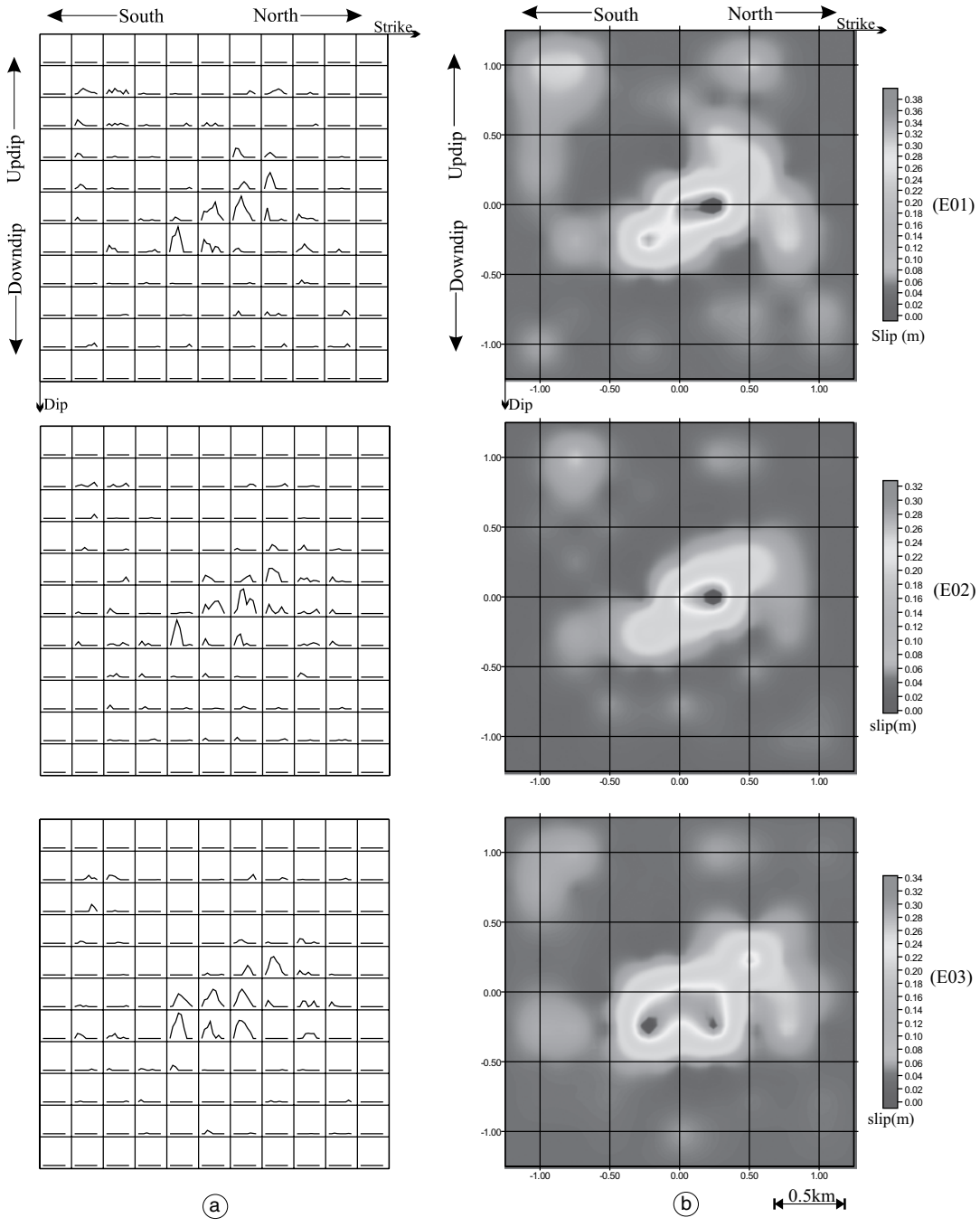

Fig. 7a,b. a) The source time function for each subevent using EGFs AF1, AF2 and AF3, respectively. b) Total slip distribution models E01, E02 and E03 using EGFs AF1, AF2 and AF3, respectively.

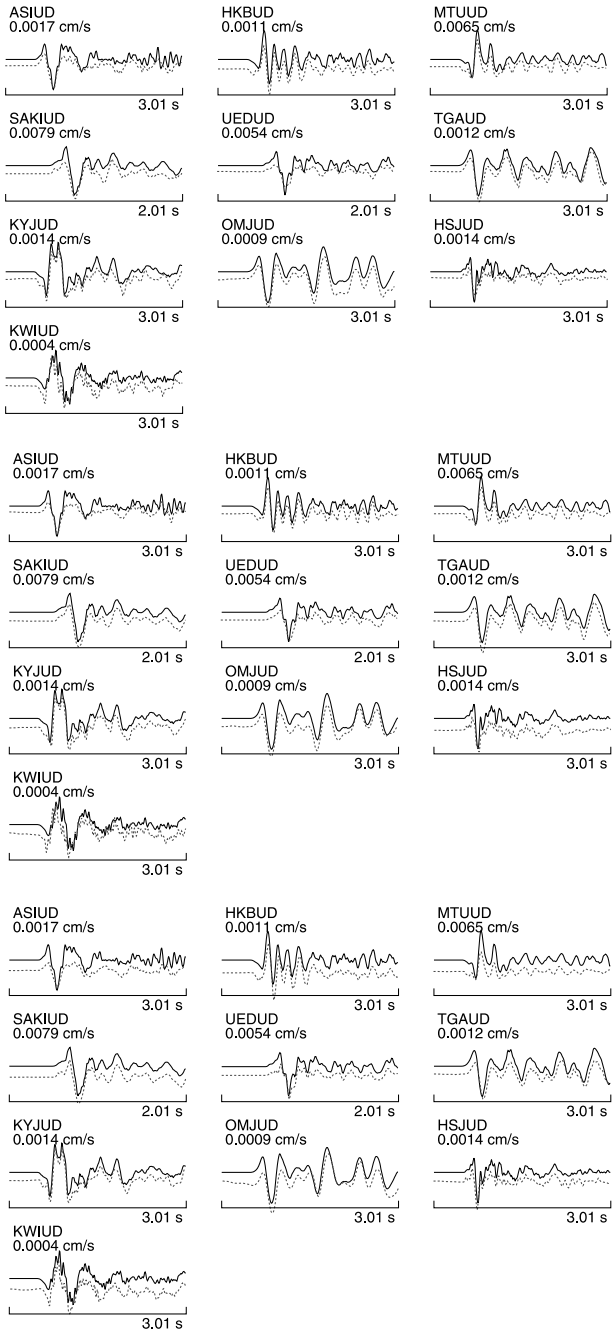

Fig. 8. Observed (solid lines) and synthetic velocity waveforms (dashed lines) of the *P*-wave records using the obtained rupture models shown in fig. 7a,b.

respectively. In general, the slip patterns are quite similar. The geometry of slip patterns is approximately elliptical. Two to three high slip patches were observed on the fault plane and can be interpreted in terms of asperities. Finally, fig. 8 shows a good comparison between the observed records and the synthetic seismograms for the obtained rupture models (fig. 7a,b). The total seismic moment is 1.74 E + 16 Nm, 1.11 E + + 16 Nm and 1.6 E + 16 Nm for E01, E02 and E03, respectively. The corresponding moment magnitude is 4.8, 4.6 and 4.7, respectively. The main result of this study indicates a complex rupture history for earthquakes of such moderate size, similar to large earthquakes.

5. Conclusions

The *P*-wave records of Nagano earthquake were analyzed in an attempt to understand the rupture behavior of moderate earthquakes. Three source rupture models of the respective event were investigated using three small aftershocks as empirical Green's functions. The distribution of aftershock and the characteristics of RSTFs were consistent with the obtained slip distribution models. The analysis of the respective study reflected that the rupture propagates bilaterally. At the first stage of rupture, RSTFs showed growth of a dynamic rupture. The set of slip models distinguished two to three high patches on the fault plane, indicating a complex rupture history. All results indicated that the investigated event occurs with a complex rupture process similar to the rupture process of large earthquakes. It could be emphasized that the detailed analysis, the set of spatio-temporal distribution of slip and the obtained RSTFs, do not reflect the so-called nucleation phase.

Acknowledgements

I would like to express my deep appreciation to S. Ide for his valuable comments and guidance. Also, I thank T. Heneda for offering his aftershock hypocentral determination. The calculations carried out at the Earthquake Research Observation, Earthquake Research Institute, University of Tokyo, Japan. Some of the figures have been generated using the Genetic Mapping Tool. I am grateful to two anonymous reviewers whose comments enhancement this study.

REFERENCES

ABDEL-FATTAH, A.K., and A. BADAWY (2001): Source process of the Southeast Beni-Suff, Northern Egypt earthquake using empirical Green's function technique, *J. Seismol.*, **6**, 153-161.

ABERCROMBIE, R. and J. MORI (1994): Local observations of the onset of a large earthquake: 28 June 1992 Landers, California, *Bull. Seismol. Soc. Am.*, **84**, 725-734.

AKAIKE, H. (1980): Likelihood and the bayes procedure, in *Bayesian Statistics*, edited by J.M. BERNARDO, M.H. DE GROOT, D.V. LINDLEY and A.F.M. SMITH (University Press, Valencia), 143-166.

ANDERSON, J. and Q. CHEN (1995): Beginning of earthquake in the Mexican subduction zone on strong-motion accelerograms, *Bull. Seismol. Soc. Am.*, **85**, 1107-1116.

ANDREWS, D.J. (1976): Rupture propagation with finite stress in antiplane strain, *J. Geophys. Res.*, **81**, 3575-3582.

BEROZA, G.C. and P. SPUDICH (1988): Linearized inversion for fault rupture behavior: application to the 1984 Morgan Hill, California, earthquake, *J. Geophys. Res.*, **93**, 6275-6296.

BRUNE, J. (1979): Implications of earthquake triggering and rupture propagation for earthquake prediction based on premonitory phenomena, *J. Geophys. Res.*, **84**, 2195-2198.

DAS, S. and C.H. SCHOLZ (1981): Theory of time-dependent rupture in the Earth, *J. Geophys. Res.*, **86**, 6039-6051.

DIBONA, M. and J. BOATWRIGHT (1989): Single-station decomposition of seismograms for subevent time histories, *Geophys. J. Int.*, **105**, 103-117.

DIETERICH, J.H. (1979): Modeling of rock friction: 1 experimental results and constitutive equations, *J. Geophys. Res.*, **84**, 2161-2168.

DIETERICH, J.H. (1986): A model for the nucleation of earthquake slip, Earthquake Source Mechanics, *Geophys. Monogr. Ser.*, edited by S. DAS, J. BOATWRIGHT and C.H. SCHOLZ, Am. Geophys. Un., Washington, **37**, 37-47.

DIETERICH, J.H. (1992): Earthquake nucleation on faults with rate and state dependent strength, *Tectonophysics*, **211**, 115-134.

ELLSWORTH, W.L. and G.C. BEROZA (1995): Seismic evidence for an earthquake nucleation phase, *Science*, **268**, 851-855.

FLETCHER, J.B. and P. SPUDICH (1998): Rupture characteristics of the three *M* 4.7 (1992- 1994) Parkfield earthquakes, *J. Geophys. Res.*, **103**, 835-854.

FRANKEL, A., J. FLETCHER, F. VERNON, L. HAAR, J. BERGE, T. HANKS and J. BRUNE (1986): Rupture characteristics and tomographic source imaging of $M_L = 3$ earthquakes near Anza, Southern California, *J. Geophys. Res.*, **91**, 12,633-12,650.

HADLEY, D.M. and D.V. HELMBERGER (1980): Simulation of strong ground motion, *Bull. Seismol. Soc. Am.*, **70**, 617-630.

HARTZELL, S.H. (1978): Earthquake aftershocks as Green's functions, *Geophys. Res. Lett.*, **5**, 1-4.

HARTZELL, S.H. and T.H. HEATON (1983): Inversion of strong ground motion and teleseismic waveform data for the fault rupture history of the 1979 Imperial Valley, California, earthquake, *Bull. Seismol. Soc. Am.*, **73**, 1553-1583.

HARTZELL, S.H. and T.H. HEATON (1986): Rupture history of the 1984 Morgan Hill, California, earthquake from the inversion of strong motion records, *Bull. Seismol. Soc. Am.*, **76**, 649-674.

IDE, S. (2001): Complex source processes and the interaction of moderate earthquakes during the earthquake swarm in the Hida-Mountains, Japan, 1998, *Tectonophysics*, **334**, 35-54.

IDE, S. and M. TAKEO (1997): Determination of constitutive relations of fault slip based on seismic wave analysis, *J. Geophys. Res.*, **102**, 27,379-27,391.

IDE, S., M. TAKEO and Y. YOSHIDA (1996): Source process of the 1995 Kobe earthquake: determination of spatio-temporal slip distribution by Bayesian modeling, *Bull. Seismol. Soc. Am.*, **86**, 547-566.

IIO, Y. (1992): Slow initial phase of the *P*-wave velocity pulse generated by microearthquakes, *Geophys. Res. Lett.*, **19**, 477-480.

IIO, Y. (1995): Observation of the slow initial phase generated by microearthquakes: implications for earthquake nucleation and propagation, *J. Geophys. Res.*, **100**, 15,333-15,349.

IRIKURA, K. and I. MURAMATU (1982): Synthesis of strong ground motions during large earthquakes, *Bull. Disaster Prev. Res. Inst., Kyoto Univ.*, **33**, 63-104.

KANAMORI, H. (1979): A semi-empirical approach to prediction of long-period ground motions from great earthquakes, *Bull. Seismol. Soc. Am.*, **69**, 1645-1670.

KIKUCHI, M. and Y. FUKAO (1985): Iterative deconvolution of complex body waves from great earthquakes - the Tokachi-Oki earthquake of 1968, *Phys. Earth Planet. Inter.*, **37**, 235-348.

KIKUCHI, M. and H. KANAMORI (1986): Inversion of complex body waves II, *Phys. Earth Planet. Inter.*, **43**, 205-222.

LAWSON, C.L. and R.J. HANSON (1974): *Solving Least Squares Problems* (Prentice-Hall, Englewood Cliffs., N. J.), pp. 340.

LI, Y. and C.H. THURBER (1988): Source properties of two microearthquakes in Kilauea volcano, Hawaii, *Bull. Seismol. Soc. Am.*, **78**, 1123-1132.

LI, Y., C. DOLL JR. and M.N. TOKSOZ (1994): Estimates of source time functions and associated parameters using the EGF method for the M = 1.5 to 4.5 earthquakes in the Charlevoix, Miramichi, and New Hampshire seismic zones, *Seism. Res. Lett.*, **65**, 32.

LI, Y., C. DOLL JR. and M.N. TOKSOZ (1995) Source characterization and fault plane determinations for M_{bLg} = 1.2 to 4.4 earthquakes in the Charlevoix seismic zone, Quebec, Canada, *Bull. Seismol. Soc. Am.*, **85**, 1604-1621.

MORI, J. and A. FRANKEL (1990): Source parameters for small events associated with the 1986 North Palm Springs, California, earthquake determined using empirical Green's functions, *Bull. Seismol. Soc. Am.*, **80**, 278-295.

MORI, J. and S. HARTZELL (1990): Source inversion of the 1988 upland, California, earthquake: determination of a fault plane for a small event, *Bull. Seismol. Soc. Am.*, **80**, 507-518.

MORI, J. and H. KANAMORI (1996): Initial rupture of earthquakes in the 1995 Ridgecrest, California sequence, *Geophys. Res. Lett.*, **23**, 2437-2440.

MORI, J. and K. SHIMAZAKI (1985): Inversion of intermediate period Rayleigh waves for source characteristics of the 1968 Tokachi-Oki earthquake, *J. Geophys. Res.*, **90**, 11,374-11,382.

MUELLER, C. (1985): Source pulse enhancement by deconvolution of an empirical Green's function, *Geophys. Res. Lett.*, **12**, 33-36.

NISHIGAMI, K. (1987): Clustering structure and fracture process of microearthquake sequences, *J. Phys. Earth*, **35**, 425-448.

OHNAKA, M., Y. KUWAHARA and K. YAMAMOTO (1987): Constitutive relations between dynamic physical parameters near a tip of the propagating slip zone during stick-slip shear failure, *Tectonophysics,* **144**, 109-125.

OLSON, A.H. and R.J. APSEL (1982): Finite faults and inverse theory with applications to the 1979 Imperial Valley earthquake, *Bull. Seismol. Soc. Am.*, **72**, 1969-2001.

SATAKE, K. (1989): Inversion of tsunami waveforms for the estimation of heterogeneous fault motion of large submarine earthquakes: 1968 Tokachi-Oki and 1983 Japan sea earthquakes, *J. Geophys. Res.*, **94**, 5627-5636.

SHIBAZAKI, B. and M. MATSU'URA (1998): Transition process from nucleation to high-speed rupture propagation: scaling from stick-slip experiments to natural earthquakes, *Geophys. J. Int.*, **132**, 14-30.

TAKEO, M. (1988): Rupture process of the 1980 Izu-Hanto-Toho-Oki earthquake deduced from strong motion seismograms, *Bull. Seismol. Soc. Am.*, **78**, 1074-1091.

TAKEO, M. and N. MIKAMI (1987): Inversion of strong motion seismograms for the source process of the Naganoken-Seibu earthquake of 1984, in *Mechanics of Earthquake Faulting*, edited by R.L. WESSON, *Tectonophysics*, **144**, 271-285.

TSUKUDA, T. (1980): Dynamical source process of microearthquakes deduced from *P*-waveforms and the structure of the fractured region within the crust, *D.Sc. Thesis of the University of Tokyo*, 1-139.

UMEDA, Y. (1990): High amplitude seismic waves radiated from the bright spot of an earthquake, *Tectonophysics*, **175**, 81-92.

UMEDA, Y. (1992): The height spot of an earthquake, *Tectonophysics*, **211**, 13-22.

WALED, D.J. and T.H. HEATON (1994): Spatial and temporal distribution of slip for the 1992 Landers, California, earthquake, *Bull. Seismol. Soc. Am.*, **84**, 668-691.

YOSHIDA, S. (1986): A method of waveform inversion for earthquake rupture process, *J. Phys. Earth*, **34**, 235-255.

YOSHIDA, S. (1988): Waveform inversion for rupture processes of two deep earthquakes in the Izu-Bonin region, *Phys. Earth. Planet. Inter.*, **52**, 85-101.

XIE, J., Z. LIU, R. HERRMANN and E. GRANSWICK (1991): Source processes of three aftershocks of the 1983 Goodnow, New York, earthquake: high-resolution images of small, symmetric ruptures, *Bull. Seismol. Soc. Am.*, **81**, 818-843.

(received January 11, 2002;
accepted October 25, 2002)